ANNALES
UNIVERSITATIS MARIAE CURIE-SKŁODOWSKA
LUBLIN - POLONIA
VOL. L/LI SECTIO AAA 1995/1996

Institute of Physics, M. Curie-Skłodowska University,
20-031 Lublin, pl. M. Curie-Skłodowskiej 1, Poland

EDWARD KRUPA, WIKTORIA TAŃSKA-KRUPA

6657

Influence of Bombarding 250 keV Ar^+ Ion Dose upon X-Ray Emission from Mo *Target*

Wpływ dozy jonów bombardujących Ar^+ o energii 250 keV na emisję promieniowania X z tarczy Mo

1. INTRODUCTION

In the past few decades, inner shell ionization processes have been intensively investigated. Most of experimental data was obtained for light ions (mainly protons) and for K-shell ionization. In the last decade, one could observe the extension of scientific interest and measurements to ions heavier than protons and to the L and M-shells. The number of L-shell experimental data has almost doubled within the recent few years. Compilations of experimental L-shell X-ray production and ionization cross sections for proton and light ion impact have been given in [1] and discussed in an overview article [2]. The available data for the M-shell can be found in [3, 4].

The measurements of L- and M-shell X-ray production cross sections in the X-ray energy region ($E_{X_{ray}} < 5$ keV) are associated with serious experimental difficulties. Besides the problems connected with determining the X-ray efficiency of a Si(Li) detector in this low energy region, the inability to resolve the X-ray spectral lines and the interference in characteristic M-shell X-ray spectra from K- and L-shell X-rays of contaminants in the targets —

the dose of bombarding ions needed to obtain a reasonably good statistics, may also have considerable influence on the data obtained experimentally. In experiments which we carried out with protons and Ar^+ ions of energy from 100–300 keV, it was observed that the emission of characteristic X-rays from the bombarded targets depends on the dose of bombarding ions previously implanted to the sample. This effect may be easily observed in a few hundred keV energy range of bombarding ions, which we shall call here *the medium — keV energy range*. Below, we mention the areas of investigation where the dose effect may have taken place.

1. L-shell ionization processes for low velocity light ions receive much attention in connection with *the low velocity effects* in L-subshell ionization. Besides the systematic discrepancies between experimental L-subshell X-ray production cross sections and ECPSSR theory, there are large deviations among experiments, depending strongly on the incident ion atomic number and energy, and the target atomic number. For low ion velocities, the errors of experimental data for L-subshell cross sections are high — the data are spread over more than an order of magnitude, which is much more than can be expected from the reported experimental errors of individual results. For example, the discrepancy in experimental and ECPSSR theory of L_2-subshell for Au bombarded α particles differs from 70% to the factor of 3.2 in different works [5–7].

2. For the reason of inability of Si(Li) detectors to resolve the X-ray spectral lines in the low energy region, the attempts at applying the wavelength dispersive methods are made. Recently, high resolution crystal spectrometers as Bragg or du Mond sets were built [8–10]. These spectrometers are one channel apparatus that, to accumulate a good statistics in one Bragg angle, need adequately long measurements, which is connected with a large ion dose gathering in the irradiated sample.

3. The method of inner-shell ionization of atoms by different slow heavy ions is interesting because of its selective property associated with level-matching effects. In [11] an attempt to determine admixtures in stainless steel with the help of 3 MeV argon ions was undertaken. The level-matching effects are the largest for bombarding ions with a few hundred keV energy. On the other hand, because of small ranges of these ions in solid, the effect of accumulation of implanted atoms under the target surface appears. This effect was observed in interaction of 250 keV Ar^+ ions with the sandwich sample of Cr/Ni on Si [12]. For a small statistics of these measurements, it is difficult to draw a conclusion about the character of the changes of X-ray emission when the dose of implanted ions increases.

In regions of investigation mentioned above, the accumulation of implanting atoms under the target surface may be considerable and may have notable influence on experimental data. The cross sections for low velocity ions are generally small, and measurements must be long, which affects in a notable ion dose absorbed in the target. Because it seemed interesting to investigate the processes which take place in medium-keV energy heavy ion-atom collisions, we have carried out an experiment in which X-rays were registered continuously when the dose of bombarding ions was increased.

In this paper, the results of investigation of L-shell X-ray emission from Mo metallic target bombarded with 250 keV Ar^+ ions are presented. Because in the registered Mo spectra the contribution of Ar K X-rays from the interaction of incident Ar^+ ions with implanted Ar atoms was observed, an additional experiment with Al target was carried out. The emitted X-rays from Mo and Al targets were registered continuously when the dose Ar^+ ions was increased up to 2.46×10^{17} Ar atoms/cm^2.

2. EXPERIMENT

The experimental setup for investigating X-rays emitted from a target bombarded with heavy ions consists of an interaction chamber presented in Figure 1, connected with the ion implanter, all set up at the Institute of Physics of the Maria Curie-Skłodowska University. Maximum energy of singly ionized ions is 300 keV.

Ar^+ ions obtained in an ion source and preliminarily accelerated to 35 keV, enter the space of 90° magnetic field, where they are analyzed with respect to their momentum. An ion beam of ^{40}Ar separated in the magnetic field was later accelerated in an acceleration tube to 250 keV. As $^{40}Ar^+$ ion beam could also contain $^{80}Kr^{2+}$ ions as the same portion of m/q, the ion currents of $^{40}Ar^+$ and $^{84}Kr^+$ were measured as equal to 38 μA and 0.035 μA, respectively. From the analysis of these ion currents and natural abundance of Kr isotopes, one could conclude that the ion current of $^{80}Kr^{2+}$ was more than four orders of magnitude smaller than for $^{40}Ar^+$. On the other hand, from our previous experiment with Kr^{2+} ions accelerated with 250 kV potential and bombarded Mo target, it follows that the production of Mo L-shell X-ray for incident Kr^{2+} ions is larger than that for Ar^+ by a factor of 2. Therefore, one may draw the conclusion that the influence of Kr^{2+} ions on production of Mo L X-rays was negligible.

The focusing and deflecting electrodes separate the ion beam from the neutral atoms of gaseous residues and direct it to the entrance aperture of

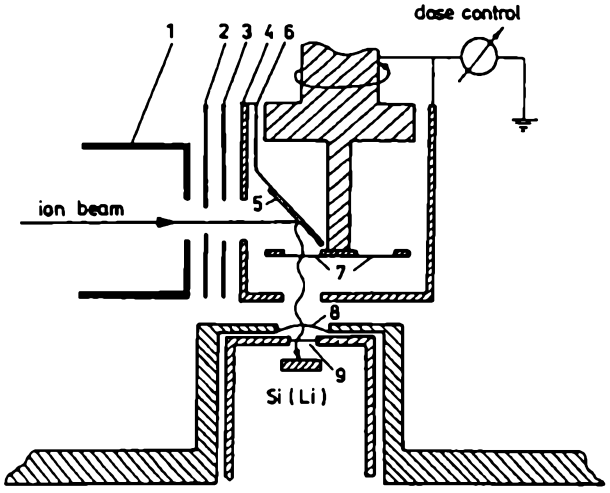

Fig. 1. The scheme of the interaction chamber for measuring X-ray induced by different ions. 1 — Faraday cup, 2 — entrance electrode with ground potential limiting the ion beam, 3 — electrode biased 500 V negative with respect to ground, 4 — secondary electron shield, 5 — experimental sample, 6 — target holder, 7 — thin (1.5 μm) mylar windows, 8 — vacuum (25 μm thick) mylar window, 9 — beryllium window of Si(Li) detector
Schemat komory oddziaływań do pomiaru promieniowania X wzbudzanego różnymi jonami. 1 — puszka Faradaya, 2 — elektroda wejściowa na potencjale ziemi ograniczająca wiązkę jonową, 3 — elektroda na potencjale −500 V względem ziemi, 4 — osłona wychwytująca elektrony wtórne, 5 — próbka badana, 6 — uchwyt próbki, 7 — cienkie (1,5 μm) okna mylarowe, 8 — próżniowe okno mylarowe o grubości 25 μm, 9 — okienko berylowe detektora Si(Li)

an interaction chamber. The diameter of the entrance aperture is 8 mm, whereas the diameter of the ion beam is considerably larger. Moreover, the ion beam is scanned in two directions — X and Y — for homogeneous irradiation of the sample.

Vacuum in the interaction chamber was obtained with a trapped (liquid-nitrogen) oil diffusion pumps, and was kept below 3×10^{-4} Pa. The sample was mounted on a fixed holder (6) and, during the experiment, it remained in the same position, inclined at 45° to the ion beam and to the Si(Li) detector axis. The sample holder was mounted to the bottom of a vessel which may be cooled with liquid nitrogen. The temperature in this vessel could be controlled during the experiment, and was kept at about 25°C. Under the sample, a thin mylar window (7) (1.5 μm thick) was placed, to protect the vacuum window (8) (25 μm thick) from the material sputtered from the target. The disc with four thin mylar windows (7) fastened to a rotative holder had the possibility to turn around the vertical axis. After each exposition, the disc was turned by 90° and another thin mylar window was

substituted under the sample. In this way, the quantity of the target material sputtered on thin mylar windows (7) and, consequently, the attenuation of X-rays in these windows, was minimized.

X-rays emitted from the sample penetrated two mylar windows (7) and (8), and a beryllium window (9) of the Si(Li) detector (6 mm in diameter). The Si(Li) detector 28 $mm^2 \times 3$ mm was located 50 mm from the center of the target. The detector resolving power was 230 eV at FWHM for 5.9 keV. The X-ray spectra obtained were stored in a multichannel analyzer connected with spectrometric devices in the CAMAC system. Before every experiment, a standard ^{55}Fe source was used for calibration purposes. A microcomputer connected through CAMAC with one channel analyzer registered continuously the intensity of X-rays emitted from the investigated sample. The integral number of counts was kept below 1500 per second to minimize a piling up of pulses registered in the Si(Li) detector.

The current and the dose of bombarding ions were measured in a summing integrator. The electrode (3) biased of 500 V negative was placed at the entrance aperture to avoid the escape of secondary electrons from the sample outside of the electron shield (4). The ion beam density was lower than 3 $\mu A/cm^2$.

3. RESULTS AND DISCUSSION

3.1. THE Mo EXPERIMENT

The 0.1 mm thick Mo metallic foil[4] manufactured by Reactor Experiments, Inc. fixed to the sample holder in the interaction chamber was bombarded with 250 keV Ar^+ ion beam 8 mm in diameter up to dose of 2.46×10^{17} Ar atoms/cm^2. [5] Figure 2 presents dependence of the numbers of Mo L and accompanying Ar K X-rays quanta upon the irradiated dose of incident 250 keV Ar^+ ions. Each point in this figure represents the number of X-ray quanta registered in the Si(Li) detector when the Mo sample was irradiated with the dose of 4.5×10^{14} Ar atoms/cm^2.

Figure 3 presents the Mo L-shell spectra measured with the Si(Li) X-ray detector. Each spectrum corresponds to 2×10^{-3} C ion fluence, which

[4] Composition of Mo sample from manufacture certificate made on the basis of chemical analysis is as follows (in percentage): Mo — 99.9847, Fe — 0.005, Cu — 0.0006, Ni — 0.0002, Cr — 0.001, Al — 0.001, Mn — 0.002, Si — 0.005, Mg — 0.0003, Ca — 0.0002.

[5] This is the dose of Ar^+ ions counted on the sample surface inclined at 45° to the ion beam direction.

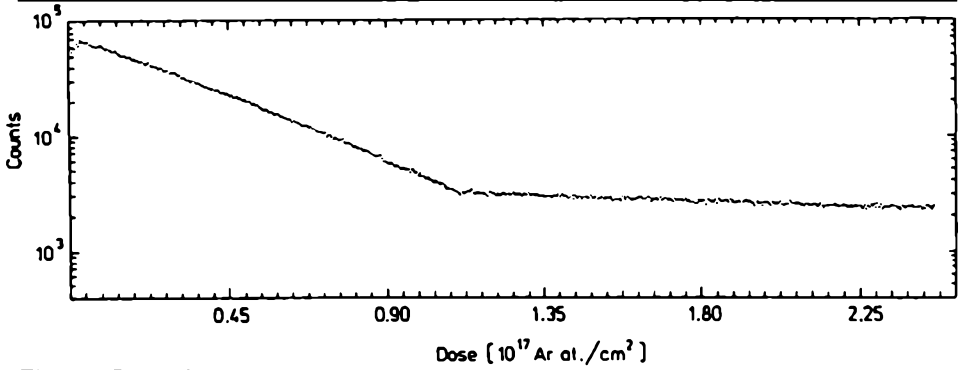

Fig. 2. Dependence of production of Mo L X-rays with the accompanied Ar K X-rays upon the dose of incident on Mo target 250 keV Ar^+ ions

Zależność natężenia promieniowania X z powłoki L Mo i towarzyszącego mu promieniowania K Ar od padającej na tarczę molibdenową dozy jonów Ar^+ o energii 250 keV

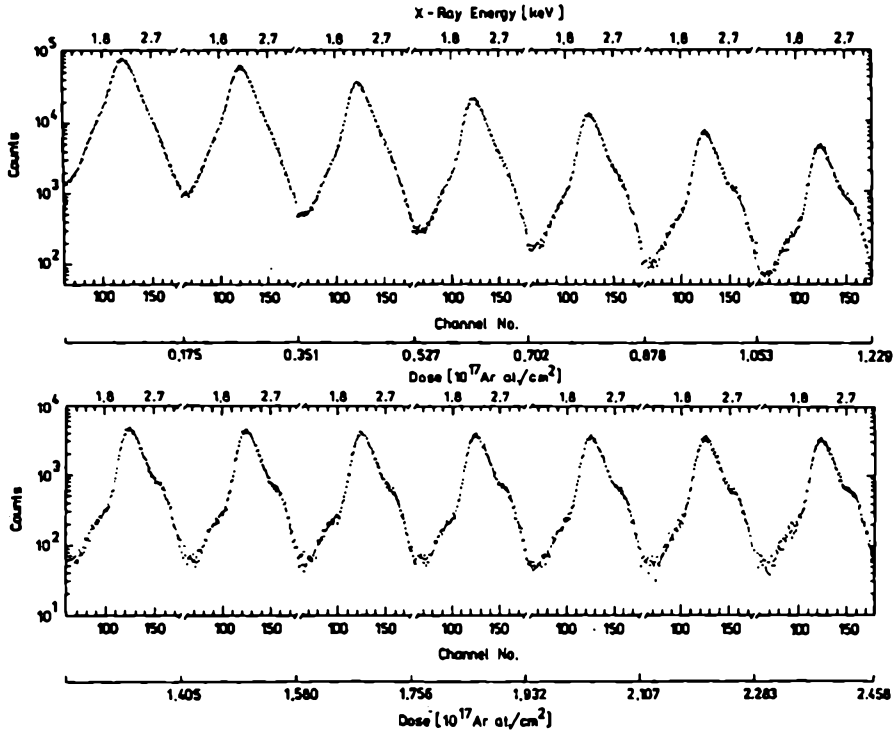

Fig. 3. Change of Mo L-shell X-ray peak with respect to irradiated dose of 250 keV Ar^+ ions in Mo target. Each spectrum is a result of 0.175×10^{17} Ar atoms/cm^2 dose

Zmiana kształtu wierzchołka promieniowania X z powłoki K Mo od dozy napromieniowania jonami Ar^+ tarczy molibdenowej. Każde widmo odpowiada dozie $0{,}175 \times 10^{17}$ at.Ar/cm^2

is equivalent to the irradiated dose of 0.175×10^{17} Ar atoms/cm^2 of the sample. After the target was irradiated with this dose, the ion beam was cut off, the disc with four thin mylar windows (7) was turned by 90°, and a new Mo L-shell spectrum, for the same sample and for the next 0.175×10^{17} Ar^+ ions/cm^2 dose, was stored in the multichannel analyzer. In this way 14 exposition presented in Figure 3 were made. The Mo sample, unchanged during all measurements, remained in the vacuum chamber. The four mylar windows (7) under the Mo sample were substituted sequentially. These thin mylar windows were used in the experiment three times and two of them, even four times. As a result of this, the sputtered material from the target was distributed on four windows, which diminished the attenuation of X-ray emitted from the target.

The main processes, which could affect experimental results were the following: the attenuation of the X-rays in the deposited on thin mylar windows material of the target, the attenuation of X-rays in the target, the sputtering erosion of the target and the diffusion of the implanted argon atoms in Mo sample.

To estimate the quantity of sample material (Mo and Al) sputtered by bombarding ions and deposited on thin mylar windows (7) located 6 mm from the center of bombarded samples, the Monte-Carlo computer simulation [13, 14] has been used. In the computer procedure, the sputtered process and the influence of previously implanted ions were taken into account. The depth profiles obtained for irradiated doses 2.4×10^{17} Ar atoms/cm^2, approximately equal to maximum experimental doses, are presented in Figure 4.

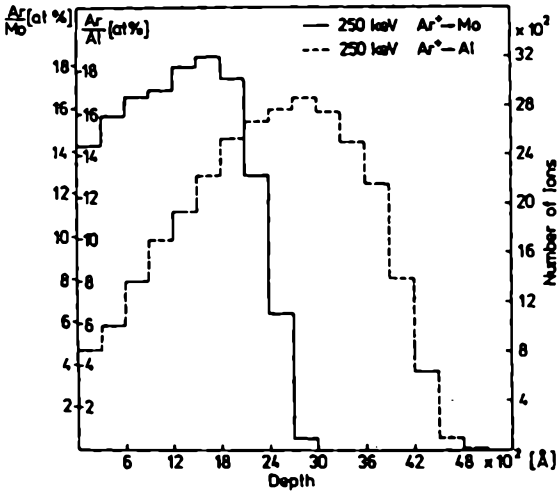

Fig. 4. Depth distributions of implanted 250 keV Ar^+ ions in Mo and Al

Rozkłady zasięgów implantowanych jonów Ar^+ o energii 250 keV w Mo i Al

The calculated sputtering ratios of Mo and Al target atoms for bombarding 250 keV Ar^+ ions are equal to 1.0 and 0.6, respectively. By simple calculations the thicknesses of the layers of sputtered target materials deposited on thin mylar windows (7) were obtained. For maximum experimental doses these thicknesses were about 180 Å for Mo and 120 Å for Al targets.

The calculations were made with the assumption that single windows were used in full Mo and Al experiments, and that the concentrations of atoms in deposited layers was equal to those in the targets. As happened in the experiments, for one fourth of these layers the attenuation of characteristic Mo L and Ar K X-ray lines increased during the experiments up to the values of about 0.2% and 0.1% for Mo and Al, respectively. In the calculation, the attenuation coefficients from [15] were used. Additional control of absorption of 3.3 keV X-rays of ^{241}Am in one of the windows after 14 expositions in Mo experiment did not show any reduction of intensity within the limits of experimental errors. The thicknesses of sputtered layers calculated from the sputtering ratios were equal to about 400 Å for Mo and 270 Å for Al targets.

The second problem is the attenuation of X-rays in the target material. X-ray production depends on the energy of ions penetrating the target. It is the largest for the initial energy of ions striking the surface layers of the target, and it decreases when the ions penetrate deeper the sample material. The formulas for X-ray yields from thick targets were given in [16–18]. An additional experiment was carried out to evaluate in our experimental conditions of the production of Mo L X-rays depending on energy of bombarding Ar^+ ions. The results of these measurements are presented in Figure 5. Each experimental point in the graph was obtained with the separate Mo target for ion fluence equal to 2×10^{-4} C. The points present the integrated number of counts in the Mo L peak normalized with regard to the ion fluence, and are expressed in counts/μC. The best fit of an analytical function to the experimental points presented in Figure 5 was obtained for:

$$P(E) = 0.0025 \cdot (E - E_{\mathrm{th}})^{2.8}, \tag{1}$$

where E is the energy of incident ions, and E_{th} is the fitting threshold energy. The value of E_{th} for Mo L X-ray production obtained from this calculation was equal to 162 keV.

The depth where the X-rays are produced in the target depending on ion energy was obtained from a Monte Carlo modified code [13]. Figure 6

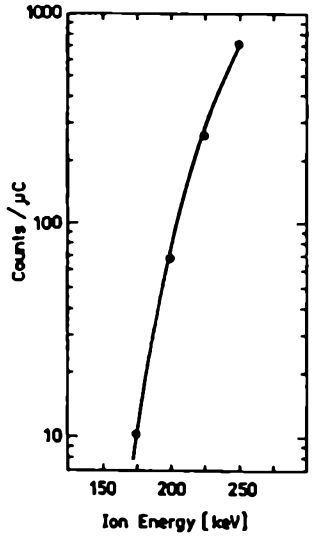

Fig. 5. Mo L-shell X-ray production as a function of the energy of Ar^+ ions
Wydajność emisji promieniowania X z powłoki Ar^+ o energii 250 keV w Mo i Al

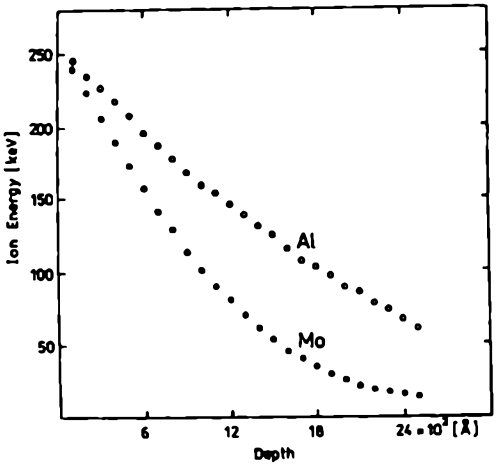

Fig. 6. Average energy of Ar^+ ions penetrating Mo target upon the distance from the surface
Średnia energia jonów Ar^+ wchodzących do tarczy Mo w zależności od odległości od powierzchni

presents average energy of Ar^+ ions penetrating Mo target[6], calculated by this program. As can be deduced from the figure, the ions reach energy E_{th} after passing the distance approximately equal to 750 Å.

To calculate the attenuation of X-rays in the Mo target material, the results presented in Figures 5 and 6 were used. As can be seen in Figure 5, the energy of ions penetrating the target and capable of producing Mo L X-rays registered in Si(Li) detector varies between the maximum experimental energy E and the threshold energy E_{th}. Each portion of energy limited by E_i and $E_i - \Delta E = E_{i+1}$, where $\Delta E = (E - E_{th})/n$, corresponds to

[6] In the calculation it was accepted that the target was inclined at 45° to the ion beam but, in the figure, on the X-axis depth is calculated perpendicularly to the surface.

a different production of X-rays $P(E_i) - P(E_{i+1}) = P_{exp}(E_i) - P_{exp}(E_{i+1}) = [P_0(E_i) - P_0(E_{i+1})]\exp(-\mu x(E_i))$ registered by the Si(Li) detector. Here, $P_0(E_i)$ is the X-ray production which would be registered in the Si(Li) detector (with its efficiency and solid angle) if the Mo target is bombarded with Ar^+ ions of energy E_i and when the attenuation in the target material is equal to zero. The part of X-ray quanta attenuated in the target material can be obtained from the following formula

$$A_{tt} = \frac{\sum_{i=1}^{n}[P(E_i) - P(E_{i+1})][e^{\mu x(E_i)} - 1]}{\sum_{i=1}^{n}[P(E_i) - P(E_{i+1})]e^{\mu x(E_i)}} \qquad (2)$$

where $x(E_i)$ is the distance which the incident Ar^+ ions penetrated in the target before they reached the average energy of E_i and μ is the total photon attenuation coefficient for Mo L X-rays [15].

Thus we have established here that the experimentally obtained dependence of X-rays production on energy of Ar^+ ions (1) represents, with a good approximation, the X-ray production yields in the Mo target material. The path x which have produced X-rays penetrated in target material was calculated by linear interpolation of Monte Carlo results presented in Figure 6 divided by cos 45°, because the target was inclined at 45 ° to the detector axis. In calculation, the attenuation of Mo L X-rays on implanted Ar atoms was not taken into account because the attenuation cross section for argon is a few times lower than that for molybdenum. A simple computer calculation has given the result for A_{tt} as <0.9%.

It is a small value not having a significant influence on the outcome of the experiments. Furthermore, the theory applied in the Monte Carlo code in general underestimates the effect of Z_1 and Z_2 oscillation for stopping power [19–21]. These oscillations are related to the level matching effects in the X-ray emission. The large values of level matching X-ray emission correspond to the large electronic stopping power cross sections. In Figure 7, the production of X-rays of some metallic targets bombarded with Ar^+ ions of energy 250 keV are presented [22]. As can be seen from this figure, the value of Z_2 oscillations of L-shell X-ray production is maximum for Nb and Mo. This means that the depths of Ar^+ ions in the Mo target is really smaller than the one calculated numerically, and the actual value of attenuation in the target material is yet lower. As was pointed out previously, the actual attenuation in thin mylar windows is also lower than it was calculated for the maximum dose, and they had negligible influence on the results of measurements. Therefore, the corrections for attenuation of X-rays in thin

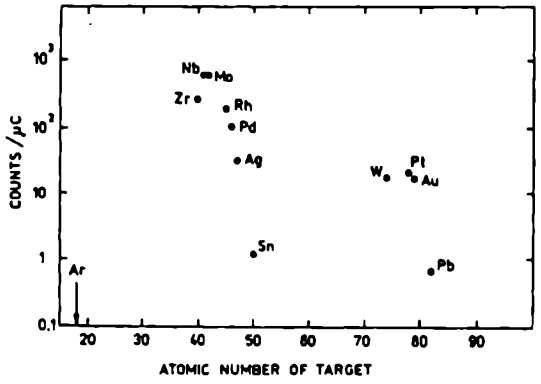

Fig. 7. Production of X-rays in incident 250 keV Ar^+ striking solid metal targets as a function of the atomic number of the target
Wydajność emisji promieniowania X wzbudzanego jonami Ar^+ o energii 250 keV w różnych tarczach metalowych w funkcji liczby porządkowej atomów tarczy

windows and in targets were not included in the resulting experimental data presented in Figures 2, 3 and 9.

The thermal diffusion of Ar atoms in the Mo target is difficult to estimate due to lack of experimental data for these components. Inert gases such as argon are applied in semiconductor technology to achieve a clean well ordered surface on a single crystal of semiconductor such as silicon. One of the standard methods of achieving clean sample surface is to sputter it with inert-gas ions and anneal at the temperature and for the time sufficient to expel the inert-gas atoms and reorder the damaged crystal. The behaviour of argon in silicon lattice after sputtering and annealing under different thermal conditions has been investigated in many works. In [23], it has been found that argon implanted at 200 keV has not been driven out from silicon by annealing temperatures as high as 1000°C. In the case of surface cleaning of silicon sputtered by Ar^+ ions in the energy range 100–1000 eV, it has been shown [24, 25] that an annealing temperature of 800°C for a period of 10 min. is needed to produce a clean and well ordered surface. Furthermore, these annealing conditions were not sufficient to remove the argon atoms which had penetrated the Si wafers, deeper than 10Å presumably as the result of channeling effects.

In our experiment, the heating of the sample by the ion beam was little, since the power delivered to the sample by the beam was about 0.4 W and the few-th grades growth of the sample holder temperature in prolonged implantation was eliminated by liquid nitrogen cooling to keep the sample in room temperature. On the basis of experimental works mentioned

above it can be concluded that the Ar atoms implanted at energy high for implantation (250 keV in our case) at room temperature are relatively immobile, particularly at the beginning of the first half of the experiment, when the irradiated dose was lower than about 1.1×10^{17} Ar atoms/cm^2 and the sample was still not highly defected.

The argon ions incoming in the Mo target (in our experiment) interact with Mo and implanted argon atoms. When their energy is larger than 162 keV, they are capable of producing X-rays registered in the Si(Li) detector. As the dose of implanted argon ions increases, the Mo target becomes an actual Mo/Ar bi-component target. The surface layers with a small concentration of implanted Ar atoms are being removed in the sputtering process. In prolonged implantation, as a consequence of the sputtering erosion process, the sample surface moves in the direction of the maximum concentration of implanted Ar atoms. The concentration of Ar atoms in layers close to the surface increases and the incoming Ar^+ ions encounter more argon atoms on their ways. In a high dose implantation due to atomic mixing, sputtering, recoil implantation the distribution of implanted Ar atoms is changing. The Monte Carlo path distribution for irradiated dose 2.4×10^{17} ions/cm^2 is presented in Figure 4. As can be seen in this figure, the concentration of argon atoms changes from 14% at the surface to 18% at the projected range R_p. The sputtering ratio of primary implanted argon ions was obtained as equal to 0.45. One can say that at this dose in the region of the Mo target, from the surface to a depth of about 0.15 μm, the concentration of argon atoms increased very slowly. For the calculation dose 1.2×10^{17} ions/cm^2, these concentrations were equal to about 7% and 11%, respectively, and the sputtering ratio for Ar atoms was 0.2.

It is explicitly seen in Figures 2 and 3 that the X-ray production from the Mo target decreases approximately exponentially with the increment of Ar^+ ion dose. The broken line in Figure 2 consists of two approximately exponential parts with different slopes. The first part with a larger slope would be associated with the X-ray emission when the concentration of Ar atoms in layers close to the surface in the Mo target was small and these layers were gradually removed in the sputtering process. The second part with a smaller exponential decrease of X-ray emission would be responsible for an approximately steady state of the Mo/Ar bi-component target. The small slope of this component would be associated with still slowly increasing concentration of Ar atoms in the amorphous high defected Ar/Mo bi-component target.

As can be seen in Figure 2, the number of emitted X-rays quanta decreases about seventeen times when the irradiated dose increased to about 1.08×10^{17} Ar atoms/cm^2 at which the steady state approach to saturation. One can say that the probability of Ar^+ ions for ionization of L-shells in Mo target atoms also decreases in the same proportion. There is smaller probability that the argon ions penetrating Mo/Ar bi-component sample material, interacting additionally with the implanted Ar atoms, would collide with Mo atoms and that the Mo L-shells would be ionized. As was proven above, the energy of Ar^+ ions in these collisions must be higher than 162 keV. This energetic condition relates also to recoiling Ar atoms. It means that the energy transferred to recoiling Ar atoms in these collisions must be relatively high, and that such events are not frequent and the ionization of Mo L shells by recoiling Ar atoms is negligibly small. As the concentration of Ar atoms in bombarded Mo target increases, the probability that argon ion loses energy in symmetrical collisions with argon atoms also increases. The probability that it encounters molybdenum atom, when its energy is still greater than E_{th}, decreases. The quantitative description of these processes needs more measurements with different ions and energy made with other targets and theoretical calculations.

From the shape of Mo L X-ray peaks presented in lower part of Figure 3, it is easy to see that each peak consists of minimum three component lines. The central and the strongest line may be attributed to the Mo L-shells lines, on the right side — the line corresponding to the Ar K X-rays and the hump appearing on the left side is connected with the detection process of low energy X-rays in Si(Li) detector [26]. It is the low energy tail of the X-ray peak, whose intensity is the larger, the smaller the difference between higher energy of registered X-rays and the Si-K absorption edge (1.839 keV).

Decomposition of Mo-Ar spectra presented in the lower part of Figure 3 was made with the help of computer program HGAM [27]. [7] The areas of Ar lines obtained from this HGAM decomposition in the last five spectra were roughly the same and equal to about 9000 within the 6% limits of experimental errors, which confirms our supposition that in steady state the concentration of Ar in the region close to surface of Mo target is constant. An example of decomposition of the last spectrum from Figure 3 is given in Figure 8.

[7] This program fits the Gaussian-peaks modified with exponential tails above the background level into the experimental X-ray spectrum. The background is fitted as polynomial of the 3rd order. In the fitted fragment of the spectrum, the maximum number of lines must not exceed 30.

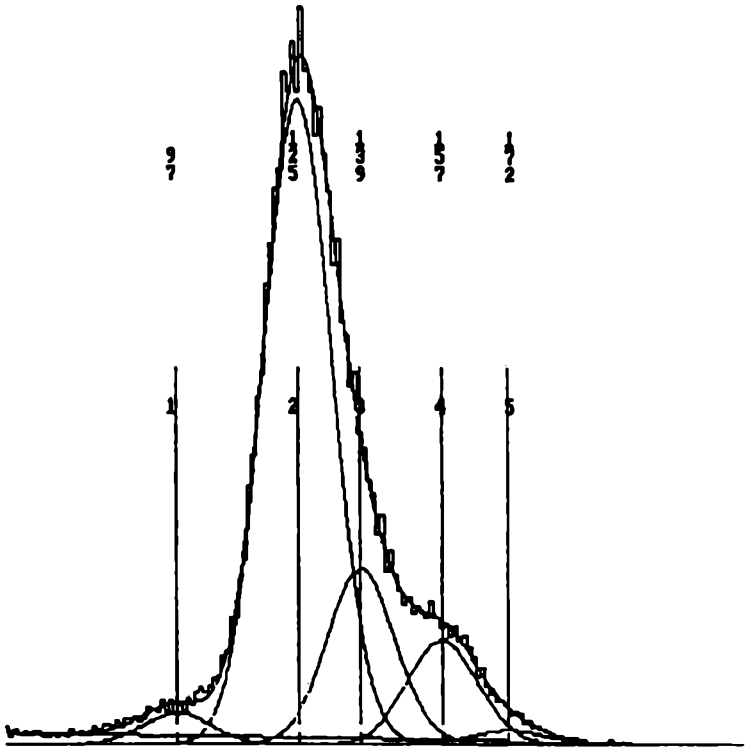

Fig. 8. Example of decomposition of the later spectra from Fig. 3 with the help of program HGAM

Przykład rozkładu ostatniego widma z ryciny 3 na składowe przy pomocy programu HGAM

3.2. THE Al EXPERIMENT

Because the Ar K and Mo L X-ray lines are not resolved in the Mo spectra, an identical experiment with Al samples was carried out to establish the presumed change of Ar K X-ray line when the dose of bombarding Ar^+ ions grew. The difference in energy of characteristic X-rays for Al K and Ar K lines is equal to about 1.5 keV, which is considerably larger than the resolving power of our Si(Li) detector. A clean Al granule[8] was rolled to 0.05 mm, rinsed in acetone and alcohol and put on the spot holder in the interaction chamber. X-ray spectra obtained in 14 parts of the experiment are presented in Figure 9. On the right side of each of them, the peak of Ar K X-ray lines is visible. The energy of the peak, which appears left to it,

[8] Composition of granulated Al material from the manufacture certificate is (in percentage): Al — 99.999; Fe, Mg — 0.0002; Cu, Cd, Pb, Na — 0.0001.

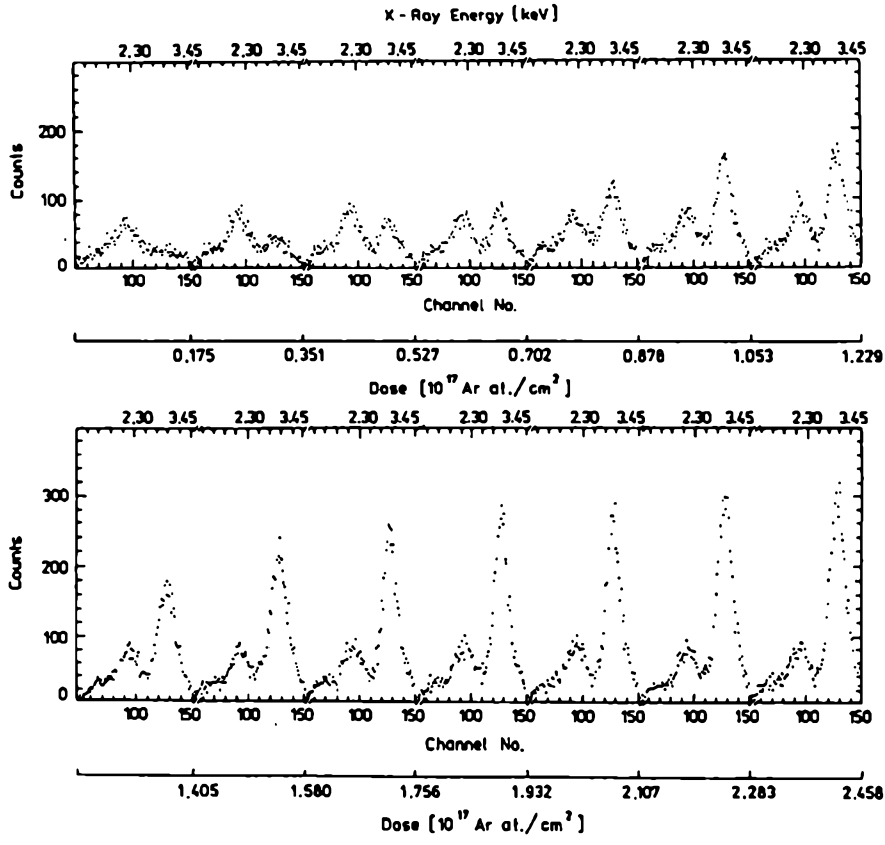

Fig. 9. Dependence of Ar K X-ray peak on irradiated dose of 250 keV Ar^+ ions striking Al target. Each spectrum was collected for the dose 0.175×10^{17} Ar atoms/cm^2
Zależności kształtu wierzchołka promieniowania X z powłoki K Ar od dozy jonów Ar^+ o energii 250 keV dla tarczy aluminiowej. Doza napromieniowania dla każdego widma wynosiła $0{,}175 \times 10^{17}$ at.Ar/cm^2

is consistent with the energy of M X-ray lines of Pb which is present as the contaminant in the Al material. A weakly marked Al K line is visible next to the left. K X-ray line of Al has registered weakly in our Si(Li) detector because of its strong attenuation in the dead layer and the beryllium window of X-ray detector and in the apparatus windows. Unfortunately, in this measurement the Al K X-ray line was partly cut off by the discriminator level in the multichannel analyzer. In another experiment with a different Al sample, the decrease of the Al K line upon the dose was also observed. We have decided to present its results because the sample which we discuss here was cleaner. As can be seen in Figure 9 the heights of

what we shall call *contaminant peaks* remain approximately constant during all measurements. This result is unexpected and it does not agree with the previously observed change of X-ray production from the target element, and which was discussed in the case with the molybdenum target. This peak intensity is also too large than it might be expected on the basis of Pb M X-ray production presented in Figure 7, and Pb concentration given by manufacturer. Another explanation is that, simultaneously with the bombarding ion beam, the contaminants with elements such as phosphorus and sulphur, which have the energy of K lines in this region, were falling on the surface of the sample. The sulphur might have come from vapours of oil from the diffusion pumps, or from contaminations of the aluminum electron shield by these elements. The chemical compounds of these two elements were used in the previous measurements and then they might appear as a consequence of secondary sputtering from the internal walls of the secondary electron shield and the thin window holder by atoms sputtered from the sample. The phosphorus might also have come from the phosphor-bronze wire spring that fastened the thin mylar window which was located a few millimeters from the bombarded aluminum sample. The sulphur and phosphorus contaminants were simultaneously ionized and sputtered from the sample surface by incident Ar^+ ions and for that reason their peak intensities remained constant. This constant intensity level of *contaminant peaks* proves that the contaminants settled on the sample surface were removed in the sputtering process and that the sample surface was continually being cleaned by incident Ar^+ ions from, e.g. the carbon from the oil of the diffusion pumps. The constant intensity level of *contaminant peaks* proves also that the observed, approximately exponential, decrease of Mo L X-ray production in Mo experiment is caused by implanted Ar atoms, not by carbon sedimented on the sample surface.

As is seen in Figure 9, the height of Ar K X-ray line increases approximately linearly with the increase of the dose of incident argon ions. It means that the production of Ar K X-ray lines increases with the increase of Ar^+ ion irradiated dose and at the maximum dose (in the present study 2.46×10^{17} Ar atoms/cm^2), it does not attain the saturation level. This result is consistent with the Monte Carlo calculations for Al target presented in Figure 4. It is seen from the calculations that the maximum range of Ar^+ ions in Al target is considerably longer than that in Mo target. The concentration of implanted Ar atoms is also spread for maximum calculation dose (2.4×10^{17} Ar atoms/cm^2) from approximately 4 to 16 per cent, which is more than it was for Mo target case. As was pointed out in [14], the

concentration of the implants in the layers from the surface to the mean projected range R_p is constant at the saturation fluence.

Approximately linear growth of Ar K X-ray production from zero proves that Ar K X-rays are emitted when Ar^+ ions collide with implanted to Al target Ar atoms. Ar K ionization does not occur when, 250 keV Ar^+ ions collide with Al atoms resting in the target.

4. CONCLUSION

Approximately exponential decrease of X-ray emission from Mo target bombarded by medium keV energy Ar^+ ions when the ion dose was strongly increased permits to make a conclusion. When the low velocity ions are used in the measurements of the ion-atom collision ionization the production of X-rays is strongly dependent on the previously implanted dose of incident particles. For the singly ionized 250 keV argon ions bombarding Mo target used in this experiment the production of L X-rays at the beginning of irradiation stayed roughly at the constant level up to the dose 1×10^{16} Ar atoms/cm^2. It was attributed to the cleaning of the sample surface from the adsorbed gaseous contaminants. Above this irradiation dose the emission of X-rays has decreased approximately exponentially with an increment of the dose up to that in which the steady state close to saturation was achieved ($\sim1.1\times10^{17}$ Ar atoms/cm^2). Further increase of the dose up to 2.46×10^{17} Ar atoms/cm^2 was leading only to a small decrease of X-rays intensity. The accompanying of the Mo L X-ray lines the ArRK X-ray line in this steady state have had approximately constant intensity.

On the contrary, the Ar K X-ray emission from the aluminum target bombarded by the argon ions of the same energy was increasing linearly with the increase of irradiation dose. The saturation state in this target was not observed up to the maximum irradiated dose, the same as for the Mo target. The results obtained experimentally are confirmed by the Monte Carlo calculations of the depth distributions. The mean projected ranges were obtained for maximum calculated doses (2.4×10^{17} Ar atoms/cm^2) equal to $\sim$ 1330 Å and $\sim$ 2440 Å for Mo and Al target respectively. Also the concentrations of implanted argon atoms in the region from surface to R_p is more differentiated in Al than Mo target.

ACKNOWLEDGMENTS

We are indebted to Prof. J. Sielanko for his help in the Monte Carlo calculation of depth distribution and modification of the program for calculating of the average energy

of Ar^+ in Mo sample. We would also like to thank K. Pyszniak and J. Liśkiewicz for their technical assistance in measurements. This work was supported by the Committee of Scientific Research, Warsaw, under Contract 2 1331 91 01.

REFERENCES

[1] Orlic I., Sow C. H. and Tang S. M., *At. Data Nucl. Data Tables*, 56 (1994) 159.
[2] Orlic I., *Nucl. Instr. and Meth.*, *B* 87 (1994) 285.
[3] Lapicki G., *Abstracts of the 16th ICPEAC*, New York, 1989, 619.
[4] Sun H. L., Kirchhoff J. F., Azordegan A. R., Duggan J. L., McDaniel F. D., Wheeler R. M., Chaturvedi R. P. and Lapicki G., *Nucl. Instr. and Meth.*, *B* 79 (1993) 186.
[5] Cai X., Liu Z. Y., Chen X. M., Ma S. X., Chen Z. C., Xu Q., Liu H. P. and Ma X. W., *Nucl. Instr. and Meth.*, *B* 72 (1992) 159.
[6] Sokhi R. S., Crumpton D., *At. Data Nucl. Data Tables*, 30 (1984) 49.
[7] Jesus A. P., Ribeiro J. P. and Lopes J. S., *J. Phys.*, *B* 20 (1987) 95.
[8] Vane C. R., Smith M., Raman S., Heard J. and Walkiewicz T., *Nucl. Instr. and Meth.*, *B* 24/25 (1987) 59.
[9] Török I., *Nucl. Instr. and Meth.*, *B* 68 (1992) 289.
[10] Lehnert U., Merla K. and Zschornack G., *Nucl. Instr. and Meth.*, *B* 89 (1994) 238.
[11] Heitz Ch., Kwadow M. and Tenorio D., *Nucl. Instr. and Meth. B*, 149 (1978) 482.
[12] Trbojevic D., Treado P. A. and Vincenz A. M., *Nucl. Instr. and Meth.*, *B* 27 (1987) 386 and 392.
[13] Sielanko J., Szyszko W., *Surf. Sci.*, 161 (1985) 101.
[14] Sielanko J., Szyszko W., *Nucl. Instr. and Meth.*, *B* 16 (1986) 340.
[15] Veigele W. M. J., *At. Data Tables*, 5 (1973) 51.
[16] Taulbjerg K., Sigmund P., *Phys. Rev.*, *A* 5 (1972) 1285.
[17] Clayton E., Cohen D. D. and Duerden P., *Nucl. Instr. and Meth.*, *B* 180 (1981) 541.
[18] Cohen D. D., Clayton E., *Nucl. Instr. and Meth.*, *B* 22 (1987) 59.
[19] Neuwirth W., Pietsch W., Richter R. and Hauser U. I., *Z. Phys.*, 275*A* (1975) 209.
[20] Kavanath T. M., Cunnigham M. E., Der R. C., Fortner R. J., Khan J. M. and Zaharis E. J., *Phys. Rev. Lett.*, 25 (1970) 1473.
[21] Land D. J., Brennan J. G., *At. Data and Nucl. Data Tables*, 22 (1978) 235.
[22] Krupa E., Tańska-Krupa W., Pyszniak K., *Ann. UMCS, AAA*, 46/47 (1991/1992) 217.
[23] Seidel T. E., Meek R. L. and Cullis A. G., *J. Appl. Phys.*, 46 (1975) 600.
[24] Margaritondo G., Rowe J. E. and Christsman S. B., *Phys. Rev.*, *B* 14 (1976) 5396.
[25] Bean J. C., Becker G. E., Petroff P. M. and Seidel T. E., *J. Appl. Phys.*, 48 (1977) 907.
[26] Inagaki Y., Shima K. and Maezawa H., *Nucl. Instr. and Meth.*, *B* 27 (1987) 353.
[27] Hanewinkel H., *Diplomarbeit, Universitaet Koeln*, Koeln 1981; Albers S., Clauberg A., Dewald A., Wesselborg C. and Zilges A., *Verhandl. DPG (VI)* 23 (1988) X, Program changed and adapted for IBM PC by J. Gręboszc, A. Maj, Z. Stachura, J. Wrzesiński, Inst. Nucl. Physics, Cracow, and D. Miskowiec, Jagiellonian Univ., Cracow.

STRESZCZENIE

W artykule przedstawiono wyniki badań emisji promieniowania X z powłoki L Mo podczas bombardowania tarczy molibdenowej jonami Ar^+ o energii 250 keV oraz emisji promieniowania X z powłoki K Ar w czasie bombardowania tarczy aluminiowej jonami Ar^+ o tej samej energii. Rejestrowano natężenie emitowanego promieniowania w zależności od dozy jonow Ar^+, od zera aż do około $2{,}5\times10^{17}$ at.Ar/cm^2. Zależność natężenia promieniowania X z powłoki L Mo od dozy jonów argonu ma, w skali połlogarytmicznej, kształt załamanej prostej o dużym nachyleniu dla małej dozy i małym nachyleniu dla dozy przekraczającej wartości $\sim1{,}1\times10^{17}$ at.Ar/cm^2. Natężenie promieniowania X z powłoki K Ar z tarczy aluminiowej wzrastało w przybliżeniu liniowo ze wzrostem dozy jonów bombardujących. W oparciu o obliczenia rozkładu zasięgów, metodą Monte Carlo, dyskutowane są obserwowane zmiany natężenia emisji promieniowania X.